Efficient Surface-Relief Gratings in Hydrogen-Bonded Polymer–Azobenzene Complexes

Arri Priimagi,*,† Klas Lindfors,† Matti Kaivola,† and Paul Rochon‡

Department of Applied Physics, Helsinki University of Technology, P.O. Box 3500, 02015 TKK, Finland, and Department of Physics, Royal Military College, P.O. Box 17000 STN FORCES, Kingston, Ontario K7K 7B4, Canada

ABSTRACT We show that efficient photoinduced surface-relief gratings can be inscribed in polymer–azobenzene complexes which are bonded by phenol–pyridine hydrogen bonding. The grating inscription was studied as a function of chromophore concentration and the molecular weight of the host polymer, both of which can be easily tuned without demanding organic synthesis. Stable gratings with modulation depth as high as 440 nm and with diffraction efficiency exceeding 40% were inscribed in the equimolar complexes. Our results demonstrate that phenol–pyridine hydrogen bonding not only allows one to increase the chromophore content until each polymer unit is occupied but is also sufficiently strong to induce mass migration of the polymer chains in a manner comparable to covalently functionalized polymers.

KEYWORDS: Azobenzene • surface-relief grating • photoinduced anisotropy • hydrogen bonding • supramolecular side-chain polymer • polymer–azobenzene complex

INTRODUCTION

Azobenzene-containing polymers have been extensively investigated because of the unique response of the azobenzene moiety to light fields (1). Their key feature is the efficient and reversible isomerization between a thermally stable trans-state and a metastable cis-state, which provides a wide range of possibilities to control the optical and photomechanical properties of the material system (2, 3). Excitation with linearly polarized light of appropriate wavelength can be used to induce large and stable in-plane anisotropy in initially isotropic azobenzene-containing films. Early studies looked at the resulting birefringence and dichroism due to orientational hole burning and photo-orientation of the chromophores perpendicular to the polarization direction of the excitation light (4, 5). The large index modulation enables efficient recording of volume-birefringence gratings, providing a pathway toward optical information processing and holographic recording (6, 7).

Perhaps the most astonishing feature of azobenzene-containing polymers is the fact that photoinduced motions of the nanometer-sized chromophores can lead to large-scale mass migration of the polymer chains over periods of several micrometers (8, 9). When exposed to an interference pattern of light with spatial variation of the intensity and/or polarization, high-modulation-depth surface-relief gratings (SRGs) can be inscribed at the polymer–air interface. This peculiar photomechanical effect holds promise for holographic applications as well as for the inscription of diffractive optical elements (10, 11). Furthermore, SRGs can be erased with light, which enables their use as wavelength-tunable output couplers in organic distributed-feedback lasers (12). Recently, SRGs have also been successfully used to direct and control the alignment of microphase separated block copolymer nanostructures, providing an interesting connection between optical alignment techniques and functional nanomaterials (13).

Light-induced surface-relief formation is a complicated process whose mechanism is not well understood (14, 15). The inscription rate and the modulation depth depend on various factors, such as the size and concentration of the azobenzene chromophores, the molecular mass of the polymer chains, and the polarization of the recording beams (16–18). Moreover, it has been generally accepted that efficient SRG formation requires strong bonding between the chromophores and the polymer chains, which has confined the majority of the studies to covalently functionalized polymers. Indeed, only very weak surface-relief structures have been inscribed in conventional guest–host type polymers (19, 20). We note, however, that light-induced surface-relief structures can also form in amorphous molecular glasses (21–23), under illumination with uniform Gaussian beams (24, 25), and when employing spiropyrans as photoactive moieties (26), which emphasizes that the basic underlying mechanism of the process is still unclear.

The most severe problems related to guest–host polymers are the low solubility of the azobenzene molecules into the polymer host and their high mobility due to the lack of bonding with the polymer. Both of these issues can be addressed by attaching the chromophores to the polymer chains through spontaneous noncovalent interactions such

* Corresponding author. E-mail: arri.priimagi@tkk.fi.
Received for review January 21, 2009 and accepted May 24, 2009
† Helsinki University of Technology.
‡ Royal Military College.
DOI: 10.1021/am9002149

as ionic bonding or hydrogen bonding (27). Such interactions enable attaching an azobenzene moiety to each repeat unit of the polymer and significantly facilitate the sample preparation compared to covalently functionalized polymers. Photoinduced motions in such polymer−azobenzene complexes have attained considerable interest in the past two years (28−33). Zhang et al. have shown that ionic complexes yield high photoinduced birefringence with impressive thermal and temporal stability (28). The photoinduced mass migration in ionic complexes has been studied by Kulikovska et al. (29, 30) They have inscribed thermally stable gratings with surface modulation depths up to 1.8 μm, demonstrating that ionic interactions can be strong enough for efficient formation of SRGs.

Compared to ionic interactions, hydrogen bonding provides some distinct advantages. First, hydrogen bonding allows for easy control over the azobenzene content, whereas in ionic complexes, cooperative binding typically leads to 1:1 stoichiometry between the constituents (34). Second, hydrogen bonding is dynamic and can be reversibly broken by external triggers. This was recently exploited by Zettsu et al., who studied SRG formation in liquid-crystalline hydrogen-bonded complexes and demonstrated that the azobenzene moieties can be selectively removed after the inscription of the gratings (31). They also showed that hydrogen bonding is essential for efficient SRG formation as no mass migration took place if the hydrogen bonding was inhibited. To the best of our knowledge, the only study on SRG formation in amorphous hydrogen-bonded polymer−azobenzene complexes has been performed by Gao et al. (32) They employed carboxyl groups to attach the chromophores to the host polymer but ran into solubility problems when using chromophores with strong electron donors. Nevertheless, they were the first to demonstrate that hydrogen bonding is strong enough to induce efficient light-initiated mass transport of the polymer.

We have recently studied the effect of chromophore concentration on the aggregation behavior and on the photoinduced anisotropy in polymer−azobenzene complexes (33, 35, 36). On the basis of our previous results, complexes employing phenol−pyridine hydrogen bonding are particularly interesting, as the chromophore concentration can be easily tuned up to the equimolar complex with no sign of macroscopic phase separation. The rationale of this work is to perform a systematic study on the applicability of phenol−pyridine hydrogen bonding for the inscription of surface-relief gratings. The complexes under investigation consist of poly(4-vinyl phenol) and 4-(2-Pyridylazo)-*N*,*N*-dimethylaniline (PVPh(PADA)$_x$; see Figure 1). The SRG formation is shown to increase monotonically with increasing chromophore concentration. The grating inscription is further enhanced by decreasing the molecular weight of the host polymer. Moreover, the inscribed gratings were stable up to 100 °C. Altogether, the SRG formation in PVPh(PADA)$_x$ complexes is very efficient as illustrated in Figure 1.

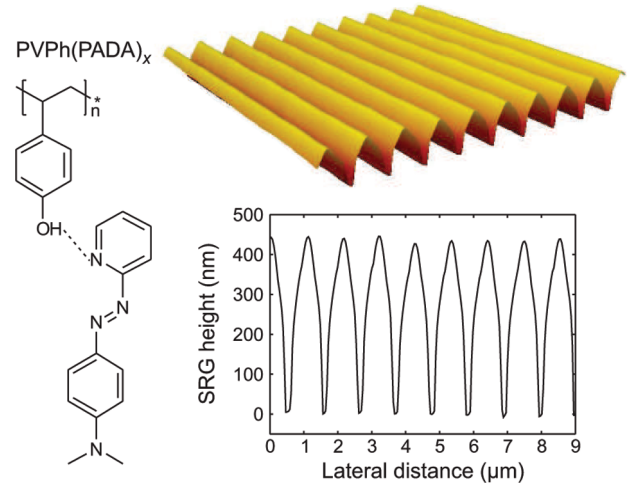

FIGURE 1. On the left: Chemical structure of the nominally stoichiometric complex PVPh(PADA)$_{1.0}$. The dashed line depicts the phenol−pyridine hydrogen bonding, which is the dominant interaction between the compounds. On the right: Atomic force microscope view (top) and surface profile (bottom) of a grating recorded on PVPh(PADA)$_{1.0}$. The M_w of the host polymer is 1000−5000 g/mol.

EXPERIMENTAL SECTION

We prepared a series of samples of PVPh(PADA)$_x$ with the degrees of complexation $x = 0.1$, 0.25, 0.5, and 1.0, which correspond to chromophore weight percentages of 16, 32, 48.5, and 65 wt %, respectively. PVPh was purchased from Sigma-Aldrich (M_w = 20 000 and 11 000) or from Maruzen Co. (M_w = 1000−5000) and PADA (purity 98%, M_w 226 g/mol) from Tokyo Kasei. The constituents were used without further purification. These were dissolved separately in tetrahydrofuran and mixed to obtain the desired degree of complexation. The solutions were stirred for 24 h, filtered through 0.2 μm syringe filters, and spin-coated onto glass substrates. All complexes yielded optically high-quality thin films with no sign of macroscopic phase separation or liquid-crystalline textures, as verified by polarized-light microscopy (Leica DM4500P). The film thicknesses were varied between 400 nm ($x = 1.0$) and 960 nm ($x = 0.1$) in order to maintain approximately constant optical density at the writing wavelength. The transmission spectra of the thin films were measured with PerkinElmer Lambda 950 spectrophotometer. Prior to optical investigations, the samples were heated to 60 °C for at least 12 h in order to remove the residual solvent. The infrared spectra were measured from samples drop cast on KBr pellets with a Nicolet 380 FTIR spectrometer by averaging 64 scans at a resolution of 2 cm^{-1}.

The recording of the gratings was performed with a spatially filtered *p*-polarized beam from a $\lambda = 457$ nm diode-pumped solid-state laser with intensity of 200 mW/cm^2. The interference pattern was created using the Lloyd mirror configuration (8): half of the beam was incident on the sample, and the other half was reflected from a mirror set at right angle with the sample to coincide with the direct beam. The fringe spacing Λ is determined by the angle between the beam propagation axis and the sample normal θ as $\Lambda = \lambda/(2\sin\theta)$. Here, the spacing was set to approximately 1.1 μm. The inscription of the gratings was monitored with a low-power (<0.5 mW) s-polarized 633 nm He−Ne laser normally incident on the sample. At this wavelength the optical density of the samples is negligible and the probe beam was not observed to affect the inscription process. The diffraction efficiency is the ratio of the power of the first-order diffracted beam to the power of the beam transmitted through an unexposed spot on the sample. The modulation depth was determined with an atomic-force microscope (Veeco Dimension 5000 SPM). The thermal stability of the gratings was studied by attaching the inscribed gratings on a heating stage

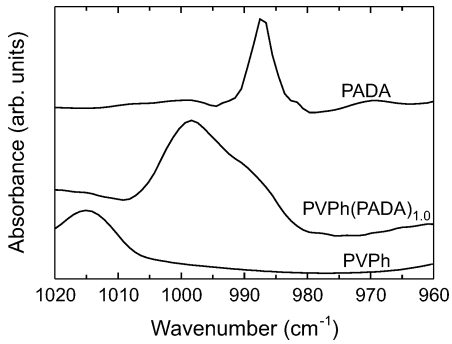

FIGURE 2. Infrared absorption spectra of PVPh, PADA, and PVPh-(PADA)$_{1.0}$ in the wavenumber region 1020−960 cm^{-1}. For clarity, the spectra are vertically shifted with respect to one another.

and monitoring the changes in the first-order diffraction efficiency upon heating of 2 °C/min. To eliminate the modulation of the signal due to interference effects caused by thermal expansion of the glass substrate, we used a low-coherence-length probe consisting of a bandpass-filtered Xenon-lamp (central wavelength 600 nm, fwhm 10 nm, intensity <1 mW/cm^2).

The thermal relaxation rate of the cis-isomer was measured by exciting the chromophores with a circularly polarized pump beam (λ = 457 nm, 40 mW/cm^2) for 10 s and monitoring the subsequent transmittance changes caused by cis−trans isomerization for 15 min. Photoinduced dichroism was studied by exciting the chromophores with an s-polarized pump beam (λ = 457 nm, 10 mW/cm^2) for a period of 500 s and by following the thermal relaxation for another 300 s. The transmittance was probed with a fiber-coupled tungsten lamp using a bandpass filter (central wavelength 530 nm, fwhm 10 nm). The transmitted signal was detected with a photodiode and a lock-in amplifier. For the dichroism measurements, the transmitted light was divided into two orthogonal polarizations using a polarizing beam splitter and both directions were detected simultaneously. The absorbance parallel ($A_{\parallel}$) and perpendicular ($A_{\perp}$) to the excitation beam polarization were then used to determine the order parameter $S = |(A_{\parallel} - A_{\perp})/(A_{\parallel} + 2A_{\perp})|$. The optical density of the samples was fixed to approximately 0.5 at the probe wavelength (530 nm). All the measurements (SRG inscription, cis-lifetime, photoinduced dichroism) were initially performed on freshly prepared samples, but could be repeated at least over a period of several months.

RESULTS AND DISCUSSION

One of the advantages of the hydrogen-bonded polymer−dye complexes compared to covalently functionalized polymers is that the chromophore content can be easily controlled by simply adjusting the mixing ratio of the constituents. If the bonding is strong enough, the concentration can be increased at least until each polymer repeat unit is occupied. For PVPh(PADA)$_x$, the nominally stoichiometric (65 wt % chromophore concentration) degree of complexation was reached with no sign of macroscopic phase separation. The complex formation between PVPh and PADA was verified by following the symmetric stretching vibration of the free pyridyl groups at 987 cm^{-1}, which is seen to shift to 998 cm^{-1} upon complexation (Figure 2). This shift can be attributed to the phenol–pyridine hydrogen bonding (33, 37). The remaining shoulder at 987 cm^{-1} indicates that even for the equimolar complex a fraction of pyridyl groups is not hydrogen-bonded. Therefore, although

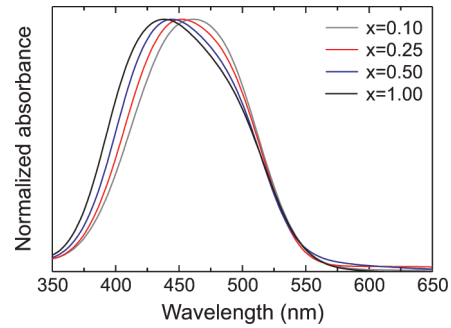

FIGURE 3. Normalized UV−vis spectra for the PVPh(PADA)$_x$ complexes.

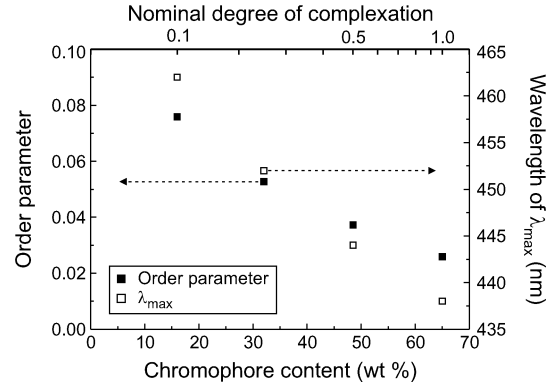

FIGURE 4. Steady-state order parameter (filled squares) and the wavelength of absorption maximum (empty squares) as a function of PADA concentration. We estimate the uncertainty in the reported order parameters to be less than ±5%.

the majority of the hydrogen bonds are between the phenol and pyridine moieties, probably also other bonds exist as both the azo group and the dimethylamino group may serve as a hydrogen-bond acceptor.

Upon increasing the degree of complexation, the UV−vis absorption maximum shifts systematically to lower wavelengths, as shown in Figure 3. The shift is in total 24 nm, from 462 nm (x = 0.1) to 438 nm (x = 1.0). Similar spectral shifts are commonly observed in azobenzene-containing systems and are typically attributed to dipole−dipole interactions between the chromophores (38−40). Such intermolecular interactions are known to affect the photo-orientation of the chromophores upon illumination with linearly polarized light, even if their role is highly dependent on the particular material system (33, 38, 41). Figure 4 presents the steady-state order parameter for PVPh(PADA)$_x$. Upon increasing the degree of complexation, the order parameter decreases systematically from 0.076 (x = 0.1) to 0.026 (x = 1.0). This decrease follows the spectral shift of the absorption maximum, also plotted in Figure 4, indicating that chromophore−chromophore intermolecular interactions decrease the angular mobility of the chromophores. We also note that the induced anisotorpy is not stable in any of the complexes. For instance, for x = 1.0, the order parameter drops rapidly from 0.026 to 0.010 once the irradiation is ceased. Moreover, saturation of the birefringence makes the bulk birefringence grating disappear in a relatively short time (42). Hence, the contribution of bulk birefringence gratings

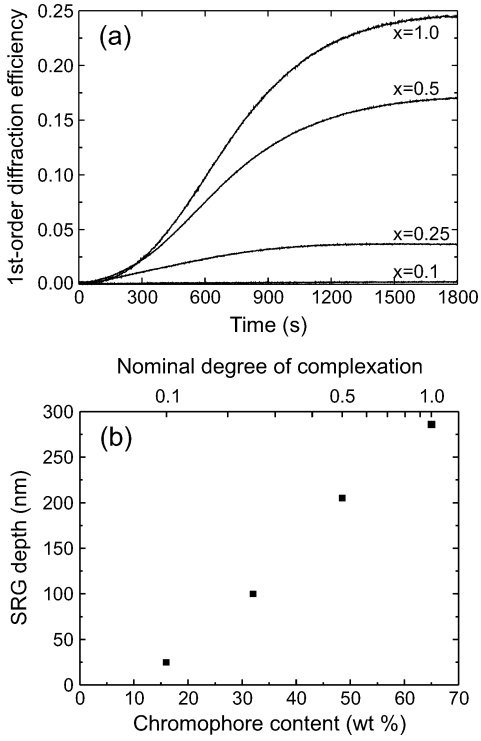

FIGURE 5. Growth of the first-order diffraction efficiency (a) and surface modulation depth (b) of the PVPh(PADA)$_x$ complexes as a function of chromophore content. We estimate the uncertainty in the SRG depth due to point-to-point variations and inhomogeneities in the beam profile to be 10%. The M_w of PVPh is 20 000 g/mol.

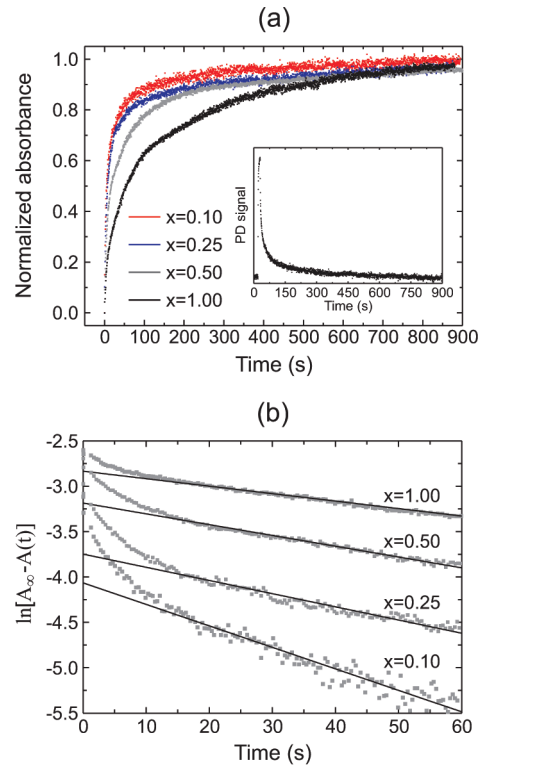

FIGURE 6. (a) Thermal cis−trans relaxation curves of the PVPh-(PADA)$_x$ complexes. The absorbance is normalized as $(A - A_0)/(A_\infty - A_0)$, where A_0 is the absorbance when the pump irradiation is turned off and A_∞ is the steady-state absorbance. The inset shows a pump/relax curve for the PVPh(PADA)$_{0.1}$ complex, where the pump is turned on and off at 20 and 30 s, respectively. (b) Plots of $\ln[A_\infty - A(t)]$ as a function of time. The slopes of the linear fits were used to determine the rate constants of thermal isomerization.

can be neglected when considering the diffraction efficiency of the inscribed surface-relief gratings.

For PVPh(PADA)$_x$, well-defined surface-relief gratings could be inscribed in each complex. As shown in Figure 5, both the first-order diffraction efficiency and the modulation depth of the gratings increase monotonically with the chromophore content. We also inscribed a grating on a 1.6 μm thick PVPh(PADA)$_{1.0}$ sample and observed no significant differences in the modulation depth compared to the thinner (400 nm) sample. Hence we conclude that the observed trend is not caused by differences in the film thickness of the samples, which is in correspondence with literature results (9, 18). The results shown in Figure 5 differ from previous studies performed with covalently functionalized polymers (18, 41, 43). Fukuda et al. have observed that in methacrylic azobenzene-functionalized side-chain polymers, the depth of surface modulation is constant above a threshold concentration of approximately 40−50 wt %. On the other hand, it has also been reported that there exists an optimum degree of functionalization, on the order of 75 mol %, above which the efficiency of SRG formation decreases. Börger et al. attributed this to the decrease of the trans−cis−trans isomerization rate at high concentrations, caused by chromophore−chromophore intermolecular interactions (41).

Efficient trans−cis−trans isomerization is an essential prerequisite for light-driven mass migration and hence the thermal lifetime of the cis-isomer is anticipated to play a role in the SRG formation. We measured the thermal relaxation rate for PVPh(PADA)$_x$ and observed a significant decrease in the relaxation rate with increasing chromophore content as shown in Figure 6a. We estimated the values of the rate constants for the complexes by fitting a linear function to the plot of $\ln[A_\infty - A(t)]$ and by neglecting the contribution of the "anomalous" fast component commonly observed in glassy polymers below T_g (44, 45). The obtained fits are shown in Figure 6b, yielding rate constants of $(23.7 \pm 0.5) \times 10^{-3}$ s^{-1}, $(14.5 \pm 0.3) \times 10^{-3}$ s^{-1}, $(11.5 \pm 0.2) \times 10^{-3}$ s^{-1}, and $(8.2 \pm 0.1) \times 10^{-3}$ s^{-1} for $x = 0.1$, 0.25, 0.5 and 1.0, respectively. However, based on the results shown in Figures 5 and 6, the increased cis-lifetime does not seem to inhibit efficient SRG formation.

The results shown in Figure 6 are in apparent contradiction with previous studies performed with azobenzene-functionalized polymers (45, 46). Barrett et al. have observed that the thermal cis−trans isomerization rate in Disperse Red 1-functionalized side-chain polymers is accelerated at high chromophore concentrations. Similar results have been obtained in dilute solutions of azobenzene-containing polymers by Haitjema et al. These results suggest that in general, steric crowding along the polymer backbone and the resulting excitonic coupling enhance the rate of thermal isomerization. We tentatively attribute the converse trend observed in PVPh(PADA)$_x$ as follows: The formation of intermolecular hydrogen bonds between the phenol and the azo moieties is known to lower the activation energy of the thermal cis−trans isomerization (47). Similarly, the rate constant can

be enhanced by complexing the azo group with weakly acidic compounds (46). In the present case, the excess of the phenolic hydrogen-bond donors at low chromophore contents results in multiple hydrogen bonds in the material system, while at high concentrations the majority of the hydrogen bonds are formed between the phenol and pyridine moieties. Hydrogen bonding at the amino functional group is expected to raise the activation barrier for isomerization, which would lead to a lower rate constant at low chromophore content instead of the trend observed here (46, 48). We therefore suggest that the tendency of the rate constant to enhance at high chromophore content is overwhelmed by the interactions between the free phenol groups and the azo groups, leading to the trend shown in Figure 6.

We also studied the role of the molecular weight (M_w) of the host polymer on the grating inscription process. This has been previously studied for azobenzene-functionalized (pDR1A) polymers blended with nonfunctionalized PMMA (17). It was found that the M_w of the blended PMMA greatly affects both the modulation depth and the inscription rate of the SRGs, and that the mass migration was absent in high-M_w blends because of polymer chain entanglement. For azobenzene-functionalized polymers, SRGs can be inscribed even if M_w exceeds 500 000 g/mol, although the inscription is less efficient than for low-M_w polymers (10). The M_w dependence of SRG formation in azobenzene-functionalized polymers was recently studied in detail over a wide M_w range (49). It was shown that high M_w reduces the inscription rate and also results in a lower modulation depth of the gratings. The effect was much smaller than anticipated, although a clear decreasing trend with increasing M_w was observed.

The diffraction efficiency for three PVPh(PADA)$_{1.0}$ complexes with different M_w of PVPh are shown in Figure 7a. Both the inscription rate and the diffraction efficiency increase significantly as the M_w of PVPh is reduced. The corresponding grating depths for the molecular weights of 20 000, 11 000, and for a polydisperse PVPh with M_w of 1000−5000 are approximately 285, 330, and 440 nm, respectively. Moreover, all the gratings were found to be stable: after blocking the writing beam, the diffraction efficiency either remained constant or increased slightly, as shown in Figure 7. We attribute the slight increase to changes in the refractive index caused by thermal cis−trans-isomerization or to optically induced chemical processes such as cross-linking or crystallization (50). Altogether, in the present hydrogen-bonded complexes, the molecular weight of the host polymer affects strongly the grating inscription process, even in the relatively narrow M_w range studied in this work. On the basis of the earlier studies described in the previous paragraph, the observed trend is predictable but stronger than expected. Now a question of great interest is whether the SRG inscription can still be enhanced by further decreasing the M_w of the host polymer. On the basis of the recent results of Ando et al., this may well be the case: they showed that the SRG formation in amorphous molecular glasses can be far more efficient than in a corresponding polymer (51).

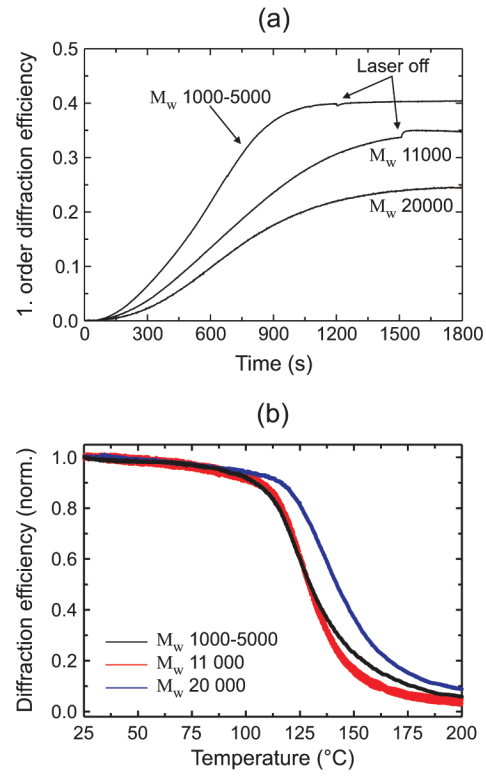

FIGURE 7. (a) Growth of the first-order diffraction efficiency and (b) the thermal stability characteristics of the inscribed gratings of PVPh(PADA)$_{1.0}$ for different molecular weights of PVPh.

Finally, we studied the thermal stability of the inscribed gratings. As shown in Figure 7b, the onset of thermal erasure for the equimolar complexes is at temperatures somewhat above 100 °C irrespective of M_w. This is an important detail, as it implies that one can enhance the SRG inscription by lowering the M_w of the host polymer without significantly compromising the thermal stability of the gratings. We note that the diffraction efficiency did not go to zero in any of the samples even when heated to 200 °C, and AFM studies verified that the SRGs could not be completely erased by heat treatment. This is related to chemical modifications of the material system under the relatively high-intensity irradiation. We noticed that irradiation (20−30 min, 457 nm, 200 mW/cm^2) of the equimolar complexes shifted the absorption maximum to approximately 410 nm and significantly decreased the absorbance of the samples, which can be attributed to photodegradation of the chromophores (52). Moreover, the irradiated areas became insoluble in tetrahydrofuran (and dimethylformamide), implying that the material is partially crystallized or cross-linked because of light irradiation. Overall, there are various factors that affect the thermal erasure characteristics of the present material system: the hydrogen bonds will be broken at elevated temperatures (53), the thermal treatment itself may give rise to bulk density gratings (50, 54), and the material system is chemically modified upon light irradiation. The detailed investigation of these effects is out of the scope of the present work.

CONCLUSIONS

We have systematically studied the surface-relief formation in hydrogen-bonded polymer–azobenzene complexes of poly(4-vinyl phenol) and 4-(2-pyridylazo)-*N*,*N*-dimethylaniline. The modulation depth increased monotonically with chromophore content, even though at the same time the thermal rate constant for cis−trans isomerization decreased significantly. Moreover, the molecular weight of the host polymer was observed to affect strongly the grating inscription process: the modulation depths for 20 000 g/mol PVPh and a polydisperse PVPh of 1000−5000 g/mol were 265 and 440 nm, respectively. Importantly, the decreasing molecular weight does not result in lower thermal stability of the gratings. Altogether, the grating inscription was very efficient, and modulation depths up to 440 nm were achieved.

More generally, our results highlight the fact that concepts of supramolecular materials science can have a profound impact on the design of polymer-based optical materials. Polymer−azobenzene complexes have proven to give rise to efficient and temporally stable photo-orientation and photoinduced mass migration. The spontaneous nature of noncovalent bonding significantly facilitates fundamental studies on the role of, e.g., chromophore−chromophore intermolecular interactions or of the molecular weight of the host polymer on such photoinduced motions. On the other hand, hydrogen bonding can be interesting from the point of view of potential applications. The most obvious advantage is the ease of sample fabrication and optimization of the composition of the material system, allowing, for instance, complexation of chromophores with different functionalities to the same polymer backbone. Hydrogen bonding may also provide novel functionalities through its dynamic nature: the bonds can be reversibly broken by external triggers or the chromophores can be extracted from the material system altogether. We also believe that the applicability of hydrogen bonding is by no means restricted to photoisomerization-driven processes but can make a difference in the performance of a wide range of optical materials.

Acknowledgment. A.P. acknowledges the hospitality of the Royal Military College and the Queen's University in Kingston, Ontario, and the Finnish National Graduate School for Materials Physics, Finnish Cultural Foundation, and Magnus Ehrnrooth Foundation for financial support. We thank F. J. Rodriguez for discussions and A. Soininen and N. Chekurov for assistance with atomic-force microscopy.

REFERENCES AND NOTES

(1) Rau, H. In *Photoreactive Organic Thin Films*; Sekkat, Z., Knoll, W., Eds.; Academic Press: San Diego, 2002; Chapter 1.
(2) Natansohn, A.; Rochon, P. *Chem. Rev.* **2002**, *102*, 4139–4175.
(3) Barrett, C. J.; Mamiya, J.; Yager, K. G.; Ikeda, T. *Soft Matter* **2007**, *3*, 1249–1261.
(4) Sekkat, Z.; Dumont, M. *Synth. Met.* **1993**, *54*, 373–381.
(5) Natansohn, A.; Rochon, P.; Gosselin, J.; Xie, S. *Macromolecules* **1992**, *25*, 2268–2273.
(6) Yu, Y.; Ikeda, T. *J. Photochem. Photobiol., C* **2004**, *5*, 247–265.
(7) Zilker, S. J.; Bieringer, T.; Haarer, D.; Stein, R. S.; van Egmond, J. W.; Kostromine, S. G. *Adv. Mater.* **1998**, *10*, 855–859.
(8) Rochon, P.; Batalla, E.; Natansohn, A. *Appl. Phys. Lett.* **1995**, *66*, 136–138.
(9) Kim, D. Y.; Li, L.; Jiang, X. L.; Shivshankar, V.; Kumar, J.; Tripathy, S. K. *Macromolecules* **1995**, *28*, 8835–8839.
(10) Viswanathan, N. K.; Kim, D. Y.; Bian, S.; Williams, J.; Liu, W.; Li, L.; Samuelson, L.; Kumar, J.; Tripathy, S. K. *J. Mater. Chem.* **1999**, *9*, 1941–1955.
(11) Harada, K.; Itoh, M.; Yataga, T.; Kamemaru, S. *Opt. Rev.* **2005**, *12*, 130–134.
(12) Ubukata, T.; Isoshima, T.; Hara, M. *Adv. Mater.* **2005**, *17*, 1630–1633.
(13) Morikawa, Y.; Nagano, S.; Watanabe, K.; Kamata, K.; Iyoda, T.; Seki, T. *Adv. Mater.* **2006**, *18*, 883–886.
(14) Garrot, G.; Lassailly, Y.; Lahlil, K.; Boilot, J. P.; Peretti, J. *Appl. Phys. Lett.* **2009**, *94*, 033303.
(15) Yager, K. G.; Barrett, C. J. *Macromolecules* **2006**, *39*, 9320–9326.
(16) Viswanathan, N. K.; Balasubramanian, S.; Li, L.; Tripathy, S. K.; Kumar, J. *Jpn. J. Appl. Phys.* **1999**, *38*, 5928–5937.
(17) Barrett, C. J.; Natansohn, A. L.; Rochon, P. *J. Phys. Chem.* **1996**, *100*, 8836–8842.
(18) Fukuda, T.; Matsuda, H.; Shiraga, T.; Kimura, T.; Kato, M.; Viswanathan, N. K.; Kumar, J.; Tripathy, S. K. *Macromolecules* **2000**, *33*, 4220–4225.
(19) Fiorini, C.; Prudhomme, N.; de Veyrac, G.; Maurin, I.; Raimond, P.; Nunzi, J.-M. *Synth. Met.* **2000**, *115*, 121–125.
(20) Lagugné Labarthet, F.; Buffeteau, T.; Sourisseau, C. *J. Phys. Chem. B* **1998**, *102*, 2654–2662.
(21) Nakano, H.; Takahashi, T.; Kadota, T.; Shirota, Y. *Adv. Mater.* **2002**, *14*, 1157–1160.
(22) Nakano, H.; Tanino, T.; Takahashi, T.; Ando, H.; Shirota, Y. *J. Mater. Chem.* **2008**, *18*, 242–246.
(23) Ishow, E.; Camacho-Aguilera, R.; Guérin, J.; Brosseau, A.; Nakatani, K. *Adv. Funct. Mater.* **2009**, *19*, 796–804.
(24) Ahmadi Kandjani, S.; Barille, R.; Dabos-Seignon, S.; Nunzi, J.-M.; Ortyl, E.; Kucharsky, S. *Opt. Lett.* **2005**, *30*, 3177–3179.
(25) Hubert, C.; Fiorini-Debuisschert, C.; Rocha, L.; Raimond, P.; Nunzi, J.-M. *J. Opt. Soc. Am. B* **2007**, *24*, 1839–1845.
(26) Ubukata, T.; Takahashi, K.; Yokoyama, Y. *J. Phys. Org. Chem.* **2007**, *20*, 981–984.
(27) Pollino, J. M.; Weck, M. *Chem. Soc. Rev.* **2005**, *34*, 193–207.
(28) Zhang, Q.; Bazuin, C. G.; Barrett, C. J. *Chem. Mater.* **2008**, *20*, 29–31.
(29) Kulikovska, O.; Goldenberg, L. M.; Stumpe, J. *Chem. Mater.* **2007**, *19*, 3343–3348.
(30) Kulikovska, O.; Goldenberg, L. M.; Kulikovsky, L.; Stumpe, J. *Chem. Mater.* **2008**, *20*, 3528–3534.
(31) Zettsu, N.; Ogasawara, T.; Mizoshita, N.; Nagano, S.; Seki, T. *Adv. Mater.* **2008**, *20*, 516–521.
(32) Gao, J.; He, Y.; Liu, F.; Zhang, X.; Wang, Z.; Wang, X. *Chem. Mater.* **2007**, *19*, 3877–3881.
(33) Priimagi, A.; Vapaavuori, J.; Rodriguez, F. J.; Faul, C. F. J.; Heino, M. T.; Ikkala, O.; Kauranen, M.; Kaivola, M. *Chem. Mater.* **2008**, *20*, 6358–6363.
(34) Faul, C. F. J.; Antonietti, M. *Adv. Mater.* **2003**, *15*, 673–683.
(35) Priimagi, A.; Cattaneo, S.; Ras, R. H. A.; Valkama, S.; Ikkala, O.; Kauranen, M. *Chem. Mater.* **2005**, *17*, 5798–5802.
(36) Priimagi, A.; Kaivola, M.; Rodriguez, F. J.; Kauranen, M. *Appl. Phys. Lett.* **2007**, *90*, 121103−1–3.
(37) Lee, L.-T.; Woo, E. M.; Hou, S. S.; Förster, S. *Polymer* **2006**, *47*, 8350–8359.
(38) Brown, D.; Natansohn, A.; Rochon, P. *Macromolecules* **1995**, *28*, 6116–6123.
(39) Tang, Z.; Johal, M. S.; Scudder, P.; Caculitan, N.; Magyar, R. J.; Tretiak, S.; Wang, H.-L. *Thin Solid Films* **2007**, *516*, 58–66.
(40) Reyes-Esqueda, J.; Darracq, B.; García-Macedo, J.; Canva, M.; Blanchard-Desce, M.; Chaput, F.; Lahlil, K.; Boilot, J. P.; Brun, A.; Lévy, Y. *Opt. Commun.* **2001**, *198*, 207–215.
(41) Börger, V.; Kuliskovska, O.; Hubmann, K. G.; Stumpe, J.; Huber, M.; Menzel, H. *Macromol. Chem. Phys.* **2005**, *206*, 1488–1496.
(42) Ivanov, M.; Priimagi, A.; Rochon, P. *Opt. Express* **2009**, *17*, 844–849.
(43) Andruzzi, L.; Altomare, A.; Ciardelli, F.; Solaro, R.; Hvilsted, S.; Ramanujam, P. S. *Macromolecules* **1999**, *32*, 448–454.
(44) Paik, C. S.; Morawetz, H. *Macromolecules* **1972**, *5*, 171–177.
(45) Barrett, C.; Natansohn, A.; Rochon, P. *Macromolecules* **1994**, *27*, 4781–4786.
(46) Haitjema, H. J.; Tan, Y. Y.; Challa, G. *Macromolecules* **1995**, *28*, 2867–2873.
(47) Gabor, G.; Fischer, E. *J. Phys. Chem.* **1962**, *66*, 2478–2481.

(48) Schanze, K. S.; Mattox, T. F.; Whitten, D. G. *J. Org. Chem.* **1983**, *48*, 2808–2813.
(49) Börger, V.; Menzel, H.; Huber, M. R. *Mol. Cryst. Liq. Cryst.* **2005**, *430*, 89–97.
(50) Pietsch, U.; Rochon, P. *J. Appl. Phys.* **2003**, *94*, 963–967.
(51) Ando, H.; Takahashi, T.; Nakano, H.; Shirota, Y. *Chem. Lett.* **2003**, *32*, 710–711.
(52) Galvan-Gonzalez, A.; Canva, M.; Stegeman, G. I.; Twieg, R.; Kowalczyk, T. C.; Lackritz, H. S. *Opt. Lett.* **1999**, *24*, 1741–1743.
(53) Ruokolainen, J.; Tanner, J.; Ikkala, O.; ten Brinke, G.; Thomas, E. L. *Macromolecules* **1998**, *31*, 3532–3536.
(54) Pietsch, U.; Rochon, P.; Natansohn, A. *Adv. Mater.* **2000**, *12*, 1129–1132.

AM9002149